Korean J. Soil Sci. Fert. **42**(4), 239-248(2009)

Article

Influence of the Starting Materials and Sintering Conditions on Composition of a Macroporous Adsorbent as Permeable Reactive Barrier

Doug-Young Chung[1],* Bong-Han Lee[2], and Jae-H. Jung[2]

[1]Dept. of Agricultural Chemistry Chungnam National University Daejeon
[2]SEWA ViSION Co. Ltd. Daejeon Korea

In this investigation, we observed surface morphology and porosity of a macroporous adsorbent made of Na-bentonite and Ca-bentonite as structure formation materials and grounded waste paper as macropore forming material for the development of a permeable reactive barrier to remove heavy metals in groundwater. Therefore, we selected minerals having higher cation exchange capacity among 2:1 clay minerals and other industrial minerals because sintering can significantly influence cation exchange capacity, resulting in drastic decrease in removal of heavy metals. The results showed that the increasing sintering temperature drastically decreased CEC by less than 10 % of the indigenous CEC carried by the selected minerals. One axial compressibility test results showed that the highest value was obtained from 5% newspaper waste pulp for both structure formation materials of Na-bentonite and Ca-bentonite although there were not much difference in bulk density among treatments. The pore formation influenced by sintering temperature and period contributes removal of heavy metals passing through the sintered macroporous media having different water retention capacity.

Key words: Sintering, Macroporous, Adsorbent, Permeable, Reactive barrier

Introduction

The growing awareness of long-term risks for soil, ecosystem health, and groundwater quality by the occurrence and behaviour of heavy metals in soils and natural waters which are the important sink of heavy metals has been grown due to the quality of the natural environment (Tiller, 1989; Alloway, 1995). Heavy metal migration through the unsaturated zone to underlying aquifer may adversely affect the quality of waters connected to contaminated areas. The behavior of heavy metals in soils is controlled by a number of processes, including metal cation release from contamination source materials, cation exchange and specific adsorption onto surfaces of soil particles and soil organic matter, and precipitation of secondary minerals (Manceau et al., 2000; McBride et al., 1997; McBride, 1999; Morin et al., 1999). The relative importance of these processes depends on soil composition and pH, nature and concentration of substrate and adsorbing ion (Spark et al., 1995), ionic strength and the presence of competing and complexing ions (Ikhsan et al., 1999).

In the soil and groundwater contaminated with heavy metals, remediation technologies commonly used for treatment of contaminants from environmental media include destruction or alteration of contaminants, extraction or separation of contaminants, and immobilization of contaminants. The concept of a permeable reactive barrier (PRB) which combines a passive chemical treatment zone with subsurface fluid flow management or biological treatment zone with subsurface fluid flow management as an in situ method for remediating contaminated ground water is relatively simple. Reactive material is placed in the subsurface to intercept a plume of contaminated ground water which must move through it as it flows, typically under its natural gradient, thereby creating a passive treatment system. As the contaminant moves through the material, reactions occur that transform it to less harmful (nontoxic) or immobile species. However, a potential problem with reactive barriers is the development of preferential flow pathways within the reactive material, resulting in decreasing the contact time between the dissolved contaminants and the reactive material (McMahon, 1997).

Reactive media used in permeable barriers should be compatible with the subsurface environment. That is, the media should cause no adverse chemical reactions or

Received : May 12. 2009 Accepted : June 8. 2009
*Corresponding author: Phone : +82428216739,
E-mail : dychung@cnu.ac.kr

byproducts when reacting with constituents in the contaminant plume, and should not act as a possible source of contaminants itself. The material should persist over long periods of time to keep PRB costs to a minimum. The material selected should minimize constraints on ground-water flow by not having excessively small particle size and it should not consist of a wide range of particle sizes that might result in blocked intergranular spaces (Starr, 1994; Shoemaker, et al., 1996).

Recently, there has been an increasing interest in the applications of an hollow microspheres ceramics known to be light, mechanically stable, and thermostable as filters, desiccants, insulators, and membrane reactors (Liu, et al., 2001; Jo, 1997; She and Ohji, 2003). Porous ceramics can be made by using pore-forming materials such as sawdust, starch, carbon or organic particulates (She and Ohji, 2003) into the starting powders, or by injection molding (Zhipeng, 1998), or by gelcasting(Liu, et al., 2001).

The article describes the structural analysis of a macroporous media which can be used as PRB to treat heavy metals as environmental media. To do this, we selected and examined the physico-chemical properties of several clay minerals and pore forming materials by thermal media forming technique. Porosity of porous media was investigated as a function of the composition of the starting powders and the sintering temperature.

Methods and materials

Materials Used To select the proper materials for making a macroporous adsorbent under various sintering temperature, we examined the physico-chemical properties of a couple of minerals, having relatively higher cation exchange capacity(CEC) among the secondary 1:1 and 2:1 clay minerals which were known to have strong affinity for heavy metals. The properties of the waste newspaper and the cocopeat which were added as a pore forming material into a mineral were also investigated (Table 1, 2). We also measured the changes of pH and CEC for the indigenous minerals under various sintering temperatures ranging from 25 to 1400℃ for 60 min.

Testing Method

Fabrication of A Sintered Macroporous Adosrbent (SMA) Bentonite and diatomite as a structure forming materials(SFM) and the waste newspaper and the cocopeat(coir) as a pore forming materials(PFM) selected from physico-chemical examination were grounded and pass through 0.177mm sieve (#80). The mixing ratios of SFM and PFM to make a SMA were varied to select proper porous properties in terms of porosity and pore size as permeability and adsorption capacity as removal of target heavy metal. The materials throughly mixed were uniformly packed into a square paper box (5 x 5 x 5 cm)

Table 1. Types of minerals and their chemical structures.

Minerals	Chemical structure	pH	EC	CEC
		1:5	dS m^{-1}	$cmol_c$ kg^{-1}
Perlite	Si, Al, K, Na, Fe, Ca, Mg, O	7.65	0.38	1.60
Vermuculite	(Mg, Ca, K, Fe Ⅱ)$_3$(Si, Al, Fe Ⅲ)$_4$$O_{10}$$(OH)_2$$O_4H_2O$	7.51	0.22	37.2
Zeolite	Clinoptilolite : [$(Na_2, K_2, Ca)O, Al_2O_3 \cdot 10SiO_2 \cdot 7H_2O$]	6.52	0.59	85.1
	Mordenite : [$(Na_2, K_2, Ca)O, Al_2O_3 \cdot 9SiO_2 \cdot 6H_2O$]			
Bentonite	$(Ai, Mg)_8(Si_4O_{10})_3(OH)_{10} \cdot 6H_2O$	9.20	1.78	83.2
Diatomite	Si:89.7, Al:3.7, iron oxide:1.09, Ignition loss : 3.7 %	6.85	0.48	28.3
Talc	$H_2Mg_3(SiO_3)_4$ or $Mg_3Si_4O_{10}(OH)_2$	9.14	0.39	0.45
Clay loam	35 % Clay (95 % Kaolinite, 4 % Mica)	4.76	0.16	8.5
Stone powder	Not Clear-mixed materials	9.10	0.75	5.5

Table 2. Chemical properties of the pore forming materials used in this experiment.

Sample	Source	pH	EC	CEC	Lignin	Cellulose	Hemicellulose	Ash
		1:5	dS m^{-1}	$cmol_c$ kg^{-1}	---------- % ----------			
Newspaper	Recycled paper	6.8	0.1	50	15	40	35	10
Coco Peat	Coconut husk	6.0	0.3	2	43	40	0.2	14

and sintered in a graphite furnace (TST, Korea) under eight levels of sintering temperatures ranging from 650 to 1350 ℃ with 100℃ increment and sintering times of 20, 30, 45, and 60 min after the internal temperature of the graphite furnace reached to each designated temperature. With the SMA, we measured bulk density, porosity, and axial compressibility as physical properties and pH and CEC as chemical properties for removal of Cd whether the developed SMA can be used as PRB. After taking the surface structure of the sintered minerals, the SMAs were cut into two pieces to observed the internal structure and pore distribution using Environmental Scanning Electron Microscopy(ESEM). A schematic drawing of the experimental procedures and the specific conditions of the experiment were shown in Fig. 1.

Analysis The analysis of physical and chemical properties of this experiment were followed the methods of soil analysis (Dane and Topp, 2002; Sparks, 1996). A sample pH was determined by 1:5 distilled water after a 30-min equilibration, and the CEC was determined by saturation with NH_4OAc at pH 7 and subsequent replacement of NH_4^+ by KCl extraction. All experiments were replicated three times and the results were averaged according to sigmastat.

Results and discussion

Characterization of Chemical and Physical Properties Fig. 2 shows the changes of pH and CEC for the minerals in a given sintering temperature. The pHs of the sintered minerals were gradually increased with increasing temperature except the expanding 2:1 clay mineral of Na-bentonite while CECs were rapidly decreased until the sintering temperature were reached to 800℃ and then stabilized to the lowest CEC for sintering temperature investigated in this experiment. pH generally increased with increasing sintering temperature for all

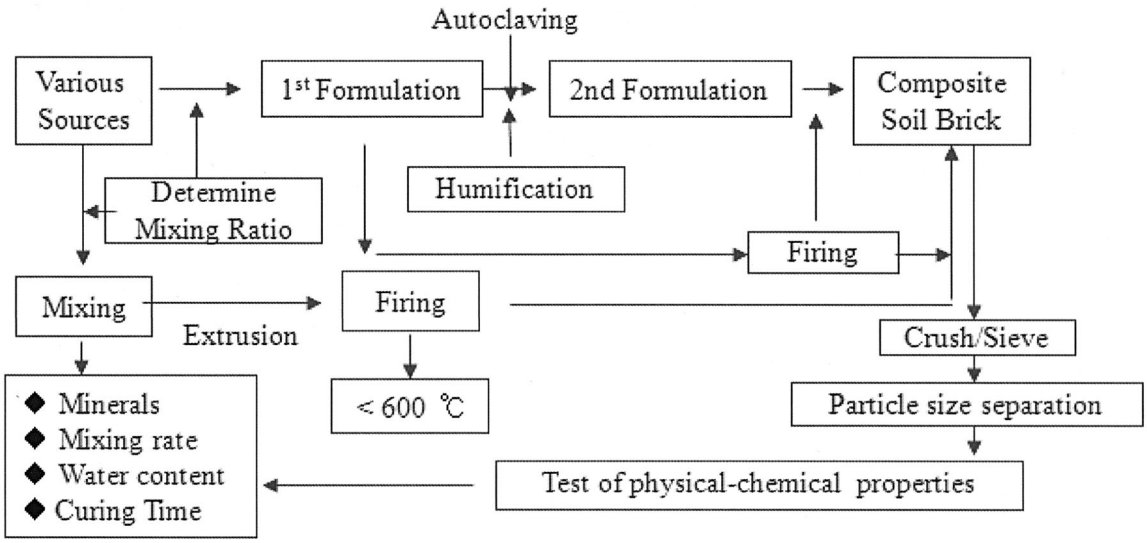

Fig. 1. Schematic procedure to develop the functional media for soil environment.

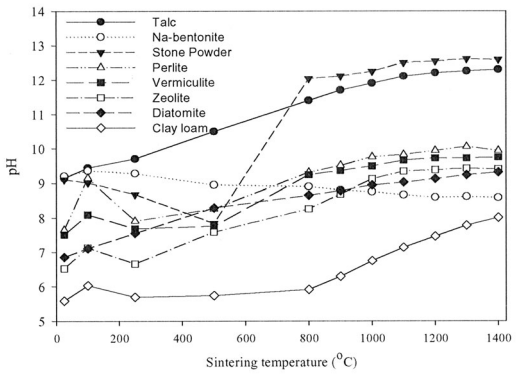

Fig. 2. Changes in pH under various sintering temperatures.

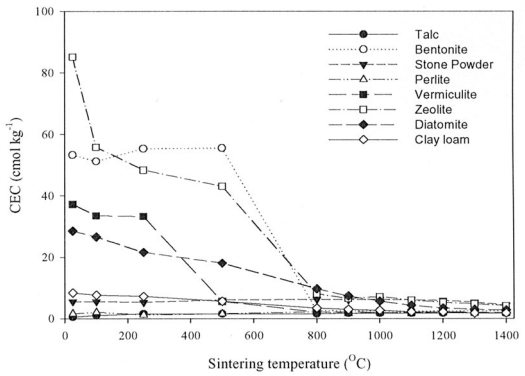

Fig. 3. Changes in CEC under various sintering temperatures.

materials selected in this experiment. The most distinctive increase in pH was 3.16 in talc while decrease in 0.62 for Na-bentonite under the same sintering temperature of 1400℃. On the contrary, decrease in CEC was distinctive for the minerals carrying initially higher CEC such as -80.96, -50.85, and -35.35 cmol kg^{-1} for zeolite, Na-bentonite, and vermiculite, respectively. This indicates that the sintering temperature significantly influenced the adsorption capacity of the minerals.

We measured the one axial compressibility of the SMA to select the proper sintering temperature in developing SMA which can be used as a PRB. As shown in Table 3, the compressibilities were higher in Na-bentonite mixed SMA than those of Ca-bentonite mixed SMA for respective PWP mixing rate, and increased with increasing amount of PWP up to 5 %. Also, the compressibility increased with increasing sintering time for the same sintering temperature. SMAs mixed with coir showed the similar results observed from SMA mixed with PWP. However, the overall compressibilities were slightly higher than those of SMA mixed with PWP.

For the SMA sintered at 950℃ which was selected to be optimum temperature based on the tests of chemical and compressibility, we measured the bulk density and porosity of the SMA. The bulk densities were slightly decreased with increasing mixing rates of PWP or coir,

Table 3. One-axial compressibility of SMA sintered at different temperature for various mixing ratios of minerals and PWP.

Mixing Ratio				intering Temp	Compressibility (kg cm^{-1})			
					Sintering Time (min)			
PWP	Coir	Na-bentonite	Ca-bentonite	(℃)	20	30	45	60
0	0	-	100	850	0.125	0.125	0.125	0.125
				950	0.250	0.250	0.563	0.750
		100	-	850	0.500	0.500	0.750	0.750
				950	1.250	1.500	1.525	1.625
2.5	-	-	97.5	850	0.250	0.250	0.50	0.753
				950	0.250	0.650	1.005	1.525
		97.5	-	850	0.250	0.250	0.350	0.525
				950	1.250	3.000	3.250	3.250
-	2.5	-	97.5	850	0.295	0.300	0.615	0.910
				950	0.325	1.125	1.350	1.450
		97.5	-	850	0.288	0.350	0.450	0.700
				950	1.438	3.500	3.725	3.750
5.0	-	-	95.0	850	0.500	0.750	1.250	1.450
				950	3.125	3.125	3.500	3.500
		95.0	-	850	1.250	1.375	1.375	1.750
				950	2.250	2.375	2.375	2.875
-	5.0	-	95.0	850	0.575	0.875	1.450	1.625
				950	3.250	3.625	3.855	4.125
		95.0	-	850	1.425	1.575	1.750	2.150
				950	3.500	3.750	3.785	4.015
7.5	-	-	92.5	850	0.500	0.625	1.500	1.725
				950	1.000	1.500	1.625	1.875
		92.5	-	850	1.000	1.250	1.750	3.000
				950	2.250	2.875	2.750	2.750
-	7.5	-	92.5	850	0.575	0.725	1.725	2.250
				950	1.150	1.725	2.250	2.750
		92.5	-	850	1.150	1.450	2.150	3.200
				950	2.725	3.325	3.450	3.650
10.0	-	-	90.0	850	0.625	1.125	1.125	1.875
				950	1.000	1.125	1.750	1.750
		90.0	-	850	1.750	2.250	2.500	3.250
				950	2.350	2.250	3.000	3.125
-	10.0	-	90.0	850	0.825	1.250	1.325	1.950
				950	1.150	1.325	2.025	2.150
		90.0	-	850	2.015	2.590	2.875	3.525
				950	2.425	2.825	3.105	3.575

Table 4. Changes in bulk density and relevant porosity for the sintered SMAs made with Na-bentonite and Ca-bentonite mixed with different amount of PWP.

Types of Mineral	Sintering Time	Amount of PWP (w/w, %)									
		0		2.5		5		7.5		10	
		BD	P	BD	P	BD	P	BD	P	BD	P
	min	g cm^{-3}		g cm^{-3}		g cm^{-3}		g cm^{-3}		g cm^{-3}	
Na-bentonite	20	0.421	0.841	0.389	0.853	0.39	0.853	0.32	0.879	0.38	0.857
	30	0.429	0.838	0.377	0.858	0.32	0.879	0.32	0.879	0.35	0.868
	45	0.431	0.837	0.384	0.855	0.37	0.860	0.30	0.887	0.37	0.860
	60	0.425	0.840	0.381	0.856	0.39	0.853	0.31	0.883	0.32	0.879
Ca-bentonite	20	0.411	0.845	0.375	0.858	0.33	0.875	0.28	0.894	0.28	0.894
	30	0.423	0.840	0.384	0.855	0.33	0.875	0.27	0.898	0.28	0.894
	45	0.432	0.837	0.364	0.863	0.30	0.887	0.27	0.898	0.28	0.894
	60	0.425	0.840	0.368	0.861	0.31	0.883	0.29	0.891	0.32	0.879

Table 5. Changes in bulk density and relevant porosity for the SMAs made with Na-bentonite and Ca-bentonite mixed with different amount of coir.

Types of Mineral	Sintering Time	Amount of PWP (w/w, %)							
		2.5		5		7.5		10	
		BD	P	BD	P	BD	P	BD	P
	min	g cm^{-3}		g cm^{-3}		g cm^{-3}		g cm^{-3}	
Na-bentonite	20	0.408	0.846	0.410	0.845	0.388	0.854	0.395	0.851
	30	0.401	0.849	0.386	0.854	0.386	0.854	0.385	0.855
	45	0.403	0.848	0.389	0.853	0.371	0.860	0.360	0.864
	60	0.400	0.849	0.410	0.845	0.372	0.860	0.360	0.864
Ca-bentonite	20	0.394	0.851	0.369	0.861	0.359	0.865	0.395	0.851
	30	0.403	0.848	0.374	0.859	0.372	0.860	0.387	0.854
	45	0.394	0.851	0.376	0.858	0.361	0.864	0.376	0.858
	60	0.386	0.854	0.372	0.860	0.355	0.866	0.369	0.861

and the lowest bulk density was obtained from 7.5 % and 7.5 to 10 % for PWP and coir mixtures, respectively. But the bulk density was generally similar within the same mixing rate (Table 4, 5). The bulk densities of SMA made with Ca-bentonite having much less swelling index were also slightly lower than those of SMA made with Na-bentonite regardless of PFMs used in this investigation.

Table 6 shows the changes in pH and CEC of SMA sintered at different temperature. As shown, pHs were slightly lower in SMAs made with Ca-Bentonite than those of SMAs made with Na-Bentonite for all PWP and sintering temperature. And pH gradually increased with increasing sintering time within the same temperature as well as pHs were also higher in higher sintering temperature. On the contrary, CEC was sharply dropped as the sintering temperature and time increased. The drastic decrease in CEC was found as the sintering period changed from 20 min to 30 min, and CEC was stabilized to the lowest in a given sintering temperature. CEC was slightly increased with increasing amount of PWP mixed. But CEC became to increase as the sintering period changes from 45 to 60 min within the same sintering temperature. For this, we assumed that sintering time significantly influenced the structure of SFM.

Sintering temperature on the structure and the pore size distributions of the specimen As preparatory test for SFM, we observed the structure change under various sintering temperature in Fig. 4. Compared the surface morphology for the indigenous minerals under room temperature, the surface morphology of the Na-bentonite, Ca-bentonite, and zeolite became loose and coarse. But voids showed up on Na-bentonite having the highest swelling index(SI). From this result, we assumed that the SFM having higher SI could be moderate mineral in development of porous media.

Fig. 5 shows the apparent surface and subsurface structure of SMA sintered for 30 and 45 min at 950℃ which was the most moderate temperature based on the compressibility test. As shown, both of surface and subsurface morphology had poor uniformity and the

Table 6. Changes in pH and CEC of SMA sintered at different temperature for various mixing ratios of minerals and PWP.

Mixing Ratio			Sintering		pH		CEC	
PWP	Ca-Bentonite	Na-Bentonite	Temp	Time	Avg.	Stdev	Avg.	Stdev
---------- % ----------			℃	mim			------ cmol kg^{-1} ---------	
0	100	0	850	20	10.58	0.11	27.40	0.54
				30	12.03	0.02	9.20	0.07
				45	12.03	0.04	9.39	0.14
				60	12.09	0.03	9.55	0.05
			950	20	11.42	1.25	20.62	0.57
				30	11.71	0.01	8.72	0.14
				45	11.59	0.08	8.98	0.09
				60	11.35	0.04	9.22	0.26
	0	100	850	20	12.28	0.01	29.82	0.62
				30	12.50	0.02	9.12	0.14
				45	13.05	0.00	9.58	0.18
				60	12.99	0.12	10.07	0.09
			950	20	12.69	0.07	19.57	0.21
				30	13.06	0.01	9.76	0.34
				45	13.01	0.05	9.09	0.14
				60	12.94	0.04	9.78	0.07
2.50	97.5	0	850	20	11.67	0.06	27.87	0.71
				30	11.75	0.01	8.89	0.69
				45	11.70	0.03	8.56	0.16
				60	11.75	0.04	9.06	0.14
			950	20	11.81	0.02	20.59	0.38
				30	11.89	0.04	8.89	0.12
				45	12.11	0.02	9.25	0.14
				60	12.49	0.06	9.33	0.12
	0	97.5	850	20	12.16	0.01	24.61	1.75
				30	12.22	0.04	11.75	0.33
				45	12.92	0.19	9.24	0.08
				60	13.05	0.04	9.02	0.18
			950	20	12.53	0.05	22.09	0.78
				30	13.11	0.01	9.36	0.11
				45	13.45	0.49	10.02	0.12
				60	13.25	0.21	9.90	0.16
5.00	95	0	850	20	12.41	0.10	22.02	0.78
				30	12.62	0.04	9.10	0.11
				45	12.81	0.00	9.52	0.12
				60	12.98	0.05	9.67	0.16
			950	20	12.81	0.04	23.74	0.21
				30	12.93	0.01	10.08	1.63
				45	12.99	0.06	10.15	0.16
				60	13.08	0.04	10.94	2.98
	0	95	850	20	12.21	0.01	26.50	0.83
				30	12.40	0.04	8.25	0.21
				45	13.11	0.00	9.17	0.28
				60	13.12	0.01	9.58	0.19
			950	20	12.90	0.01	23.46	1.41
				30	13.00	0.04	11.13	0.28
				45	13.04	0.01	11.87	0.00
				60	13.18	0.04	12.04	0.26

Table 6. continued

Mixing Ratio			Sintering		pH		CEC	
PWP	Ca-Bentonite	Na-Bentonite	Temp	Time	Avg.	Stdev	Avg.	Stdev
---------- % ----------			℃	mim			------ cmol kg^{-1} ---------	
7.50	92.5	0	850	20	12.40	0.01	30.06	0.91
				30	12.42	0.08	10.72	0.26
				45	13.02	0.04	14.05	0.49
				60	13.08	0.01	17.93	0.33
			950	20	12.31	0.02	30.53	0.24
				30	12.18	0.00	5.70	0.09
				45	12.42	0.12	6.65	0.40
				60	12.66	0.07	7.28	0.11
	0	92.5	850	20	12.31	0.01	37.02	1.82
				30	12.41	0.05	8.42	0.16
				45	12.69	0.04	10.50	0.14
				60	13.08	0.06	12.07	0.80
			950	20	12.35	0.01	33.98	0.11
				30	13.15	0.03	6.32	0.12
				45	13.11	0.04	7.36	0.14
				60	12.97	0.02	8.51	0.07
10.00	90.0	0	850	20	12.62	0.04	37.72	0.81
				30	12.76	0.02	9.76	0.40
				45	12.89	0.06	9.20	0.02
				60	13.14	0.01	9.06	0.10
			950	20	12.54	0.04	36.22	0.08
				30	12.72	0.19	8.20	0.06
				45	12.84	0.04	7.60	0.21
				60	13.09	0.05	6.81	0.16
	-	90.0	850	20	12.58	0.01	38.54	1.24
				30	13.02	0.49	10.75	0.38
				45	13.09	0.21	8.97	0.39
				60	13.11	0.10	8.37	0.35
			950	20	12.53	0.04	34.69	0.62
				30	12.74	0.00	10.79	0.71
				45	12.94	0.05	9.00	0.17
				60	13.14	0.04	6.97	0.39

surface colors and subsurface structure were influenced by types of SFM and sintering temperature. The apparent pores on the surface of SMA were observed with increasing sinteing temperature for Ca-bentonite with 10 % PWP while there were not distinctive void development for Na-bentonite with 10 % PWP. The subsurface structure changed from coarse to dense platy as the sintering period increased. This indicated that the sintering period could be important factor in formation of pores.

In Fig. 6, we observed the subsurface morphologies of SMA made of Ca-bentonite mixed with different amount of PWP. The distinctive voids were increased with increasing amount of PWP although there were not much changes in porosities as observed in Table 4. However, we interpret that the increasing sintering temperature could influence the combustion of amended PWP and fusion of minerals, resulting in crystallization of SFM.

Fig. 7 shows the pore distribution of SMA made of Na-bentonite mixed with different amount of PWP. The pores were clearly observed even on SMA of 5 % PWP amendment and the number and size of pores increased with increasing amount of PWP while the pores for SMA sintered at 850 were not uniformly distributed as well as the pores were not clearly identified, compared with SMA sintered at 950℃. This indicates that the sintering

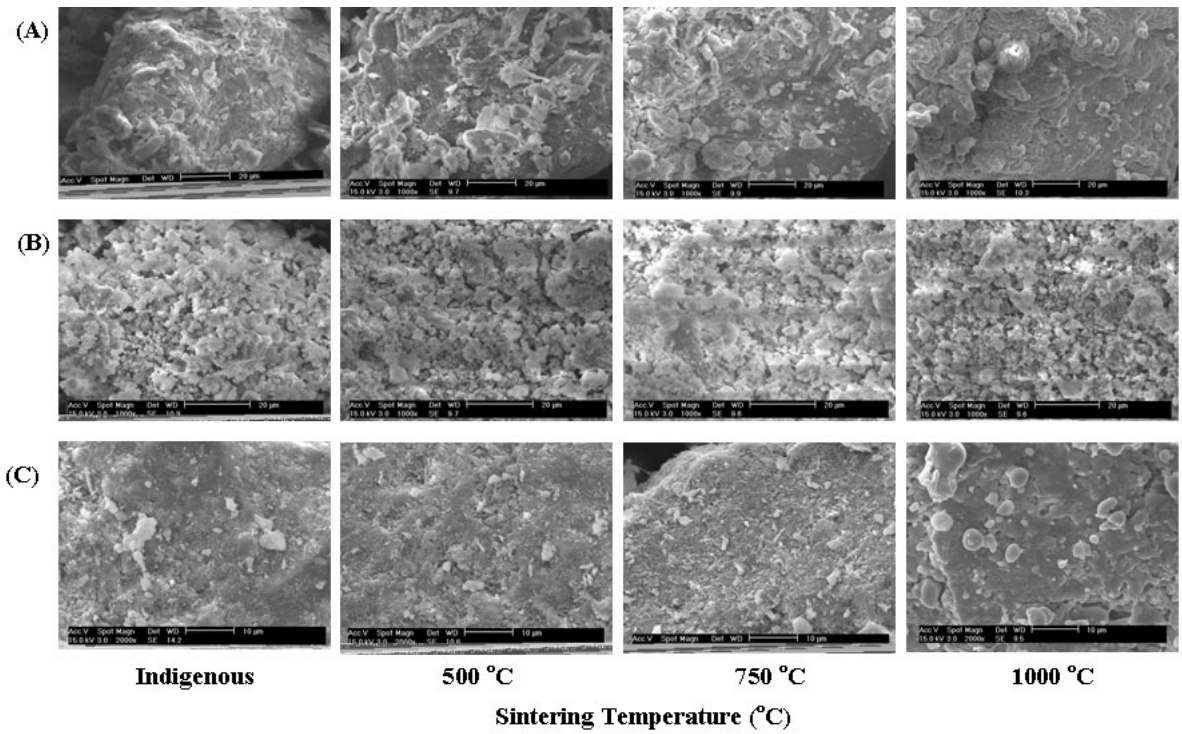

Fig. 4. ESEM images of indigenous dry PFM. (A)Ca-bentonite, (B)Na-bentonite, (C)Zeolite

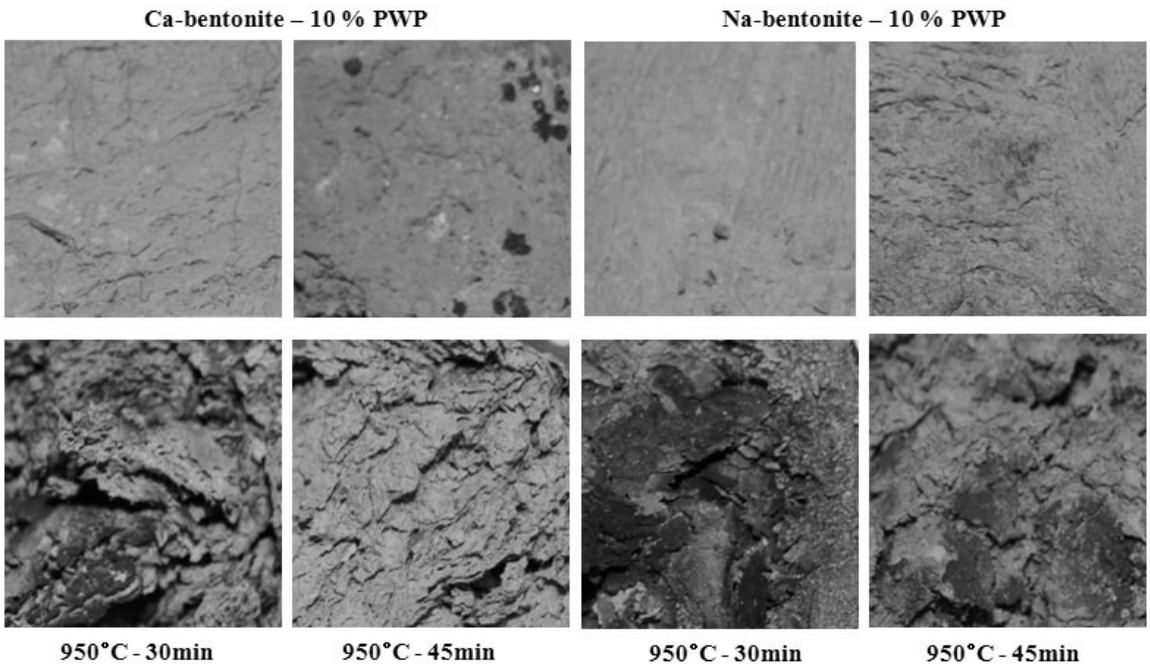

Fig. 5. Photographs of surface(top) and subsurface(bottom) structures of two types of SMA sintered for 30 and 45 min at 950℃.

temperature strongly influence the formation and distribution of pores on the subsurface of SMA.

Conclusion

Reactive macroporous media developed with aim of permeable barriers should be compatible with the subsurface environment. The chemical properties of structural forming materials were significantly influenced by the sintering temperature, resulting in drastic decrease in the adsorption capacity of the minerals. Sinteing temperature also influenced the development of apparent pores on the surface of SMA. The apparent pores on the surface was distinctive from the material showing less

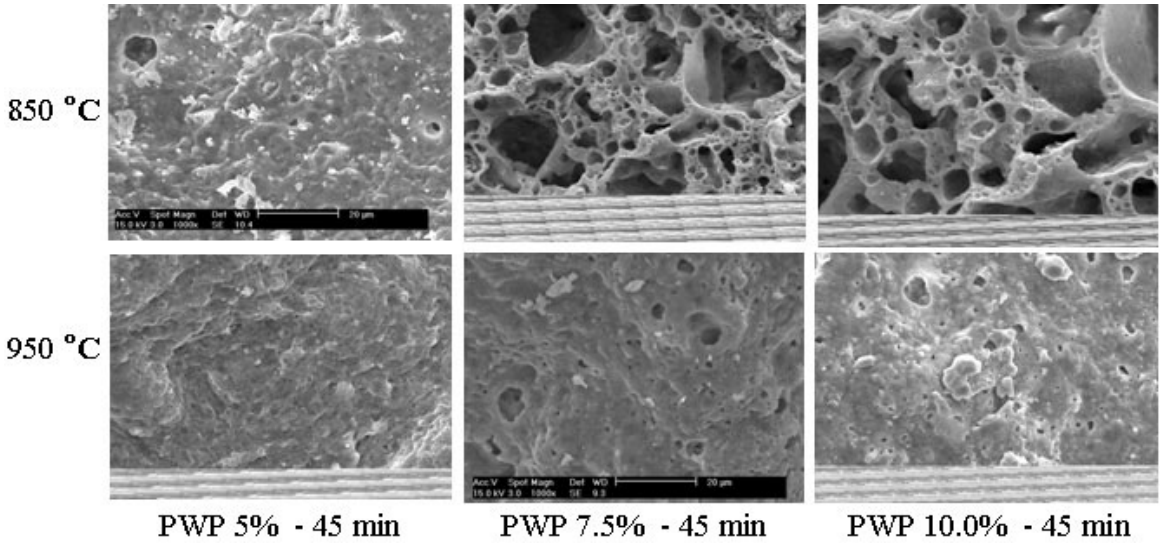

Fig. 6. ESEM images of SMA made of Ca-bentonite mixed with different rates of PWP at two different sintering temperature of 850 and 950℃.

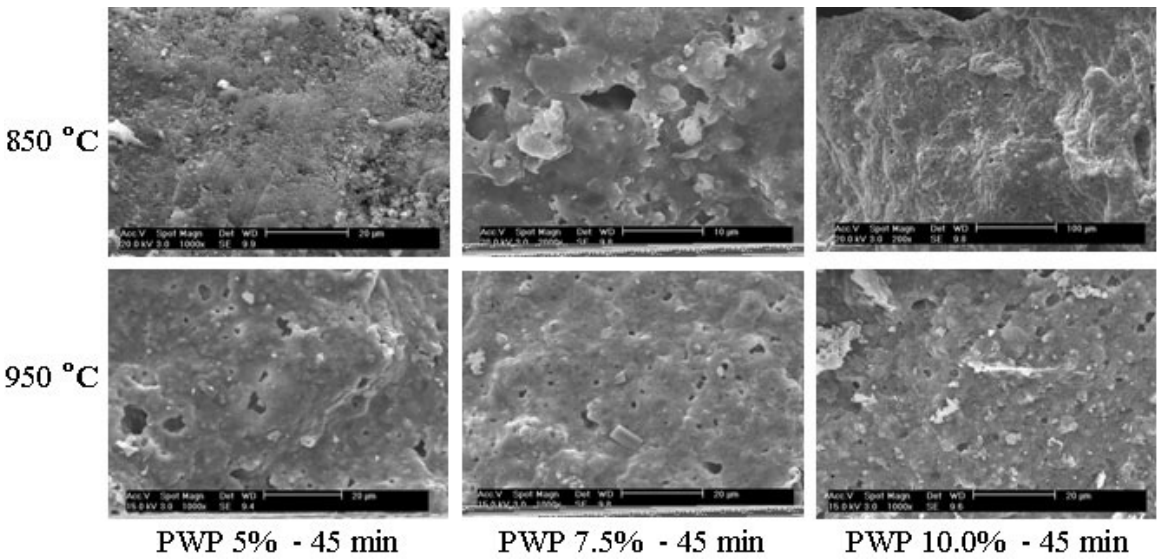

Fig. 7. ESEM images of SMA made of Na-bentonite mixed with different rates of PWP at two different sintering temperature of 850 and 950℃.

swelling index, indicating that hydrated sphere of the bentonite influenced the formation of crystallization in sintering macroporous adsorbent. With these results, we could conclude that the starting materials having less swelling capacity was favorable for development of macroporous adsorbent which can be used as permeable reactive barriers.

Acknowledgement

We appreciate to carry out this research as development project of energy and resource technology through KEMCO in 2007

References

Alloway, B.J. 1995. Heavy metals in soils. John Wiley and Sons, New York.

Deng, Z.-Y., T. Fukasawa, and M. Ando. 2001. High-surface-area alumina ceramics fabricated by the decomposition of Al(OH)3, J. Am. Ceram. Soc. 84.3. pp. 485-491.

Ikhsan, J., Johnson, B.B., and Wells, J. D. 1999. A comparative study of the adsorption of transition metals on kaolinite. Journal of Colloid and Interface Science 217, 403-410.

Jo, Y.M. 1997. Characterization of ceramic composite membrane filters for hot gas cleaning, Power Technol. 91.1. pp. 55-62.

Kabata-Pendias A. 2001. Trace elements in soils and plants. Third Edition, CRC Press, NY.

Liu, Y.F., X.Q. Liu, H. Wei, and G.Y. Meng, Porous mullite ceramics from national clay produced by gelcasting, Ceram. Int. 27 (2001), pp. 1-7.

Dane, J. H. and G. C. Topp. 2002. Methods of Soil Analysis. Part 4. Physical Methods. Part 1. 2nd ed. Agron. Monogr. 9. ASA and SSSA, Madison, WI.

Sparks, D.L. 1996. Methods of soils analysis. Part 3. SSSA Book Ser. 5. SSSA, Madison, WI.

Manceau, A., B. Lanson, M.L. Schlegel, J.C. Harge, M. Musso, L. Eybert-Berard, J.L. Hazemann, D. Chateigner, and G.M. Lamble. 2000. Quantitative Zn speciation in smelter- contaminated soils by EXAFS spectroscopy. Am. J. Sci. 300:289-343.

McBride, M.B. 1999. Chemisorption and precipitation reactions. p. B265 -B302. In M.E. Sumner (ed.) Handbook of soil science. CRC Press, Boca Raton, FL.

McBride, M.B., S. Sauve, and W. Hendershot. 1997. Solubility control of Cu, Zn, Cd, and Pb in contaminated soils. Eur. J. Soil Sci. 48:337-346.

McLaughlin, M.J., R.E. Hamon, R.G. McLaren, T.W. Speir, and S.L. Rogers. 2000. Review: A bioavailability-based rationale for controlling metal and metalloid contamination of agricultural land in Australia and New Zealand. Aust. J. Soil Res. 38:1037-1086. Soil Sci. Plant Anal. 31:1661-1700.

McMahon, P.B. 1997. "Field Evaluation of a Permeable Reactive Barrier Containing Zero-Valence Iron at the Denver Federal Center." Remediation Technologies Development Forum, Permeable Barriers Action Team meeting. Virginia Beach, Virginia.

She, J.H. and T. Ohji. 2003. Fabrication and characterization of highly porous mullite ceramics, Mater. Chem. Phys. 80. pp. 610-614.

Shoemaker, S.H., Greiner, J.F., and R.W. Gillham. 1996. "Permeable Reactive Barriers in Assessment of Barrier Containment Technologies": A Comprehensive Treatment for Environmental Remediation Applications. Rumer, R.R. and Mitchell, J.K. (eds.). U.S. DOE, U. S. EPA, and DuPont Company. pp. 301353

Spark, K.M., J.D. Wells, and B.B. Johnson. 1995. Characterizing trace metals adsorption on kaolinite. European Journal of Soil Science 46, 633-640.

Starr, R.C. and J.A. Cherry. 1994. "In situ remediation of contaminated groundwater: The funnel-and-gate system." Ground Water 32(3): 46.

Tiller, K.G. 1989. Heavy Metals in soils and their environmental significance. Advances in Soil Science 9, 114-141.

초기 소재와 소성조건이 투수반응벽체인 대공극흡착제 조상에 미치는 영향

정덕영[1,*] · 이봉한[2] · 정재현[2]

[1]충남대학교 농업생명과학대학 생물환경화학과, [2](주)세와비젼

본 실험은 지하수에 포함된 중금속을 제거하기 위한 투수성반응벽체를 개발하기 위하여 대공극 형성물질로 분쇄한 폐지와 식물섬유를 그리고 구조형성소재로 Na와 Ca-벤토나이트를 사용하여 소성 후 소성된 소재의 표면구조와 공극발달 특성을 조사하였다. 그러나 소성은 중금속 제거율을 급격히 감소시키는 양이온교환용량에 영향을 미치므로 2:1 점토광물 중에서 양이온교환용량이 큰 점토광물과 일반 산업물질을 소재를 선정하였다. 연구 결과는 살펴보면 소성온도가 증가함에 따라 소성에 사용된 소재의 기존 CEC의 10 % 이하로 급격히 감소되는 경향을 보여주었다. 일축 압축 시험 결과 처리간 용적밀도는 큰 차이가 없었지만 Na와 Ca-벤토나이트를 소성소재 모두 폐지가 5 % 정도 처리하였을 때 압축강도가 가장 높은 것으로 나타났다. 그리고 소성온도와 기간 모두 공극 형성에 영향을 미친 것으로 조사되었다. 이러한 연구 결과로부터 다공체 내에 형성된 공극은 수분 투수 특성과 중금속 제거에 모두 영향을 미칠 것이라 추정하였다.